

Circumambulatory Movement of Negative Charge (“Ring Walk”) during Gas-Phase Dissociation of 2,3,4-Trimethoxybenzoate Anion

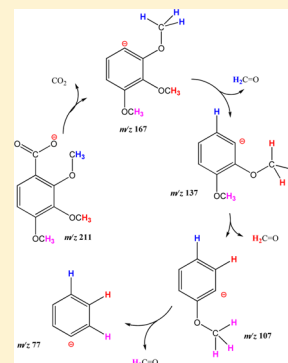
Kithsiri B. Herath,^{†,‡} Carl S. Weisbecker,[†] Sheo B. Singh,[‡] and Athula B. Attygalle^{*,†}

[†]Center for Mass Spectrometry, Department of Chemistry, Chemical Biology, and Biomedical Engineering, Stevens Institute of Technology, Hoboken, New Jersey 07030, United States

[‡]Merck Research Laboratories, Rahway, New Jersey 07065, United States

S Supporting Information

ABSTRACT: A dramatic “ortho effect” was observed during gas-phase dissociation of *ortho*-, *meta*-, and *para*-methoxybenzoate anions. Upon activation under mass spectrometric collisional activation conditions, anions generated from all three isomers undergo a CO₂ loss. Of the *m/z* 107 ions generated in this way, only the 1-dehydro-2-methoxybenzene anion from the *ortho* isomer underwent an exclusive formaldehyde loss. A peak for a formaldehyde loss in the spectra of 2,4-, 2,5-, and 2,6-dimethoxybenzoates and the absence of an analogous peak from 3,4- and 3,5-dimethoxy derivatives confirmed that this is a diagnostically useful *ortho*-isomer-specific phenomenon. Moreover, the spectrum from 2,3-dimethoxybenzoic acid showed peaks for two consecutive formaldehyde losses. The 1-dehydro-2,3,4-trimethoxybenzene anion (*m/z* 167) generated from 2,3,4-trimethoxybenzoate in this way endures three consecutive eliminations of formaldehyde units. For this, the negative charge, initially located on position 1, circumambulates to position 2, then to position 3, and finally to position 4 to form the final phenyl anion. The proposed stepwise fragmentation pathway, which resembles the well-known E1cB-elimination mechanism, is supported by tandem mass spectrometric observations made with 2-^[13C²H₃]methoxy-3-^[13C]methoxy-4-methoxybenzoic acid, and ab initio calculations. In addition, the spectra of ions such as 1-dehydro-3,4-dimethoxybenzene anion show peaks for consecutive methyl radical losses, a feature that establishes the 1,2-relationship between the two methoxy groups.

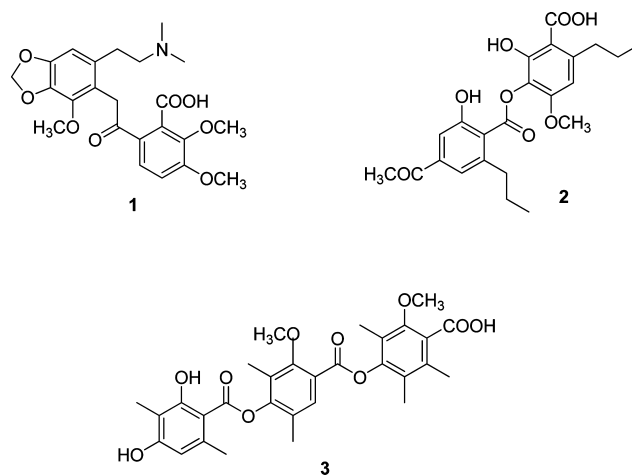


INTRODUCTION

Electrospray ionization, one of the most widely used sample introduction techniques in modern mass spectrometry, generates predominantly even-electron (EE) gaseous ions.¹ The gaseous ions generated in this way undergo little or no fragmentation because electrospray imparts only very little internal energy to ions. To obtain structural information from EE ions, they are usually mass selected by tandem mass spectrometry and subjected to collision-induced dissociation (CID). Although CID spectra often appear simple, their interpretation is not always straightforward because of many rearrangements that take place during fragmentation. Many attempts have been made to formulate fragmentation rules based on empirical observations and use artificial intelligence (AI) to interpret CID spectra of even-electron ions.^{2,3} Similar efforts have been made without much success for decades to interpret electron ionization (EI) mass spectra. Although AI approaches are successful for sequence determination of oligomeric compounds such as peptides, they offer little help for unambiguous identification of novel small molecules. Undoubtedly, before attempting to develop meaningful AI programs for the interpretation of EE spectra,² we must first thoroughly comprehend the underlying fragmentation pathways.

In the course of our explorations on fragmentation mechanisms of low-molecular-weight anions,^{4,5} we noted an *ortho*-isomer-specific loss of formaldehyde from methoxybenzoic acids isomers. Understanding the fragmentation pathways of this group of compounds is important because benzoic acid

derivatives with multiple methoxy groups are widely encountered as secondary metabolites. Some examples are narceine from fungi (1),⁶ sekikaic acid from lichens (2),⁷ and the antibiotic Thielavin B from the marine fungus *Thielavia terricola* (3).⁸ Identification of these compounds is not usually straightforward because their isolation in pure form is rather difficult. In addition, the determination of ring-substitution pattern by NMR spectroscopy is



Received: February 4, 2014

Published: April 21, 2014

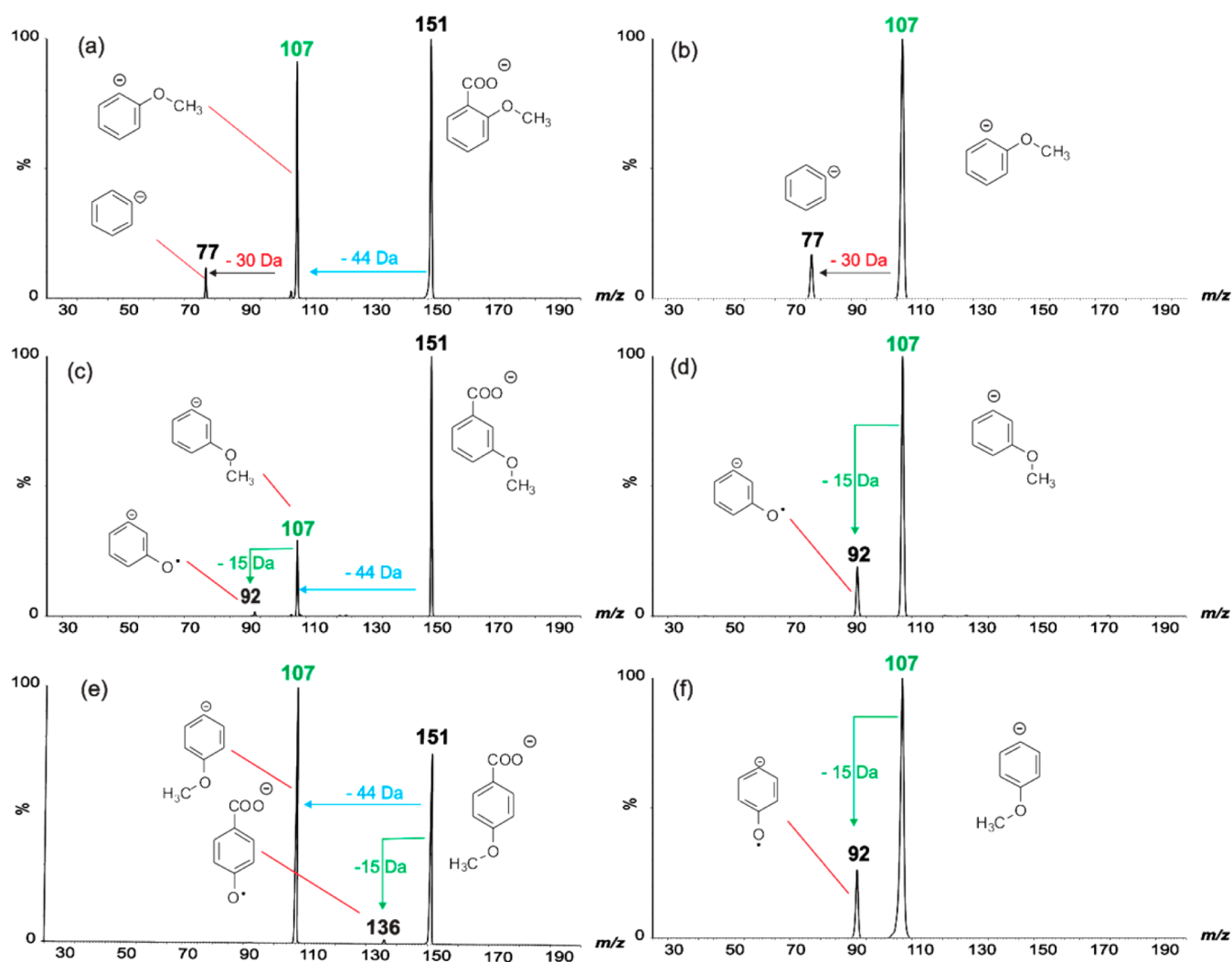
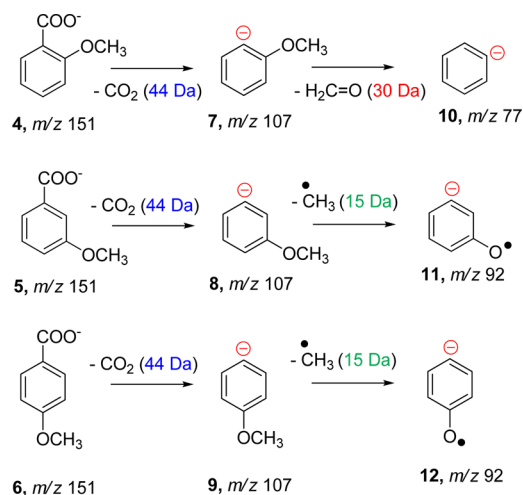


Figure 1. Unit-resolution CID mass spectra recorded from the m/z 151 anion generated from (a) *o*-, (c) *m*-, and (e) *p*-methoxybenzoic acid, and (b, d, and f) those of their respective in-source-generated m/z 107 ions at a collision energy setting of 20 eV (note: the smaller m/z 107 ion undergoes more fragmentation at 20 eV than the larger m/z 151 ion).

cumbersome due to the presence of only a few aromatic protons. In contrast, mass spectrometric analysis can be performed directly on crude mixtures.

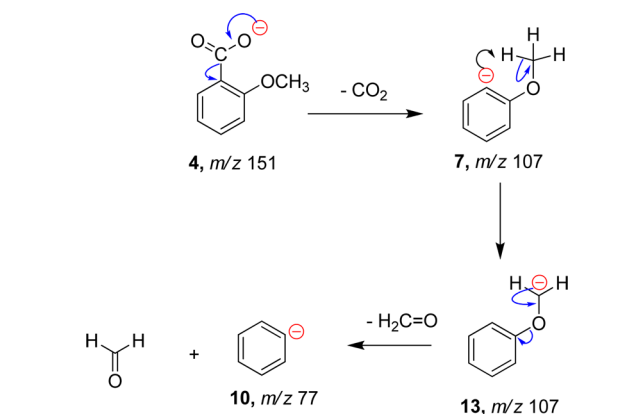
Thus, we undertook a comprehensive investigation on interpretation of CID mass spectra of congeners of methoxybenzoic acids. Our initial results showed that the negative charge of the anion, generated by the incipient decarboxylation, moves in a circumambulatory manner when the methoxy group is adjacent to the ring carbon bearing the charge. By definition, a circumambulatory rearrangement is a type of unimolecular chemical reaction in which a chemical entity undergoes a displacement around the periphery of a conjugated ring.⁹ These mechanisms are sometimes described more colorfully as a “merry-go-round” or as “ring walking” rearrangements.^{10,11} The mechanism of circumambulation is a well-debated subject in the study of gas-phase chemistry of aromatic ions. A 1,2-hydrogen shift mechanism has been proposed as one possible pathway to rationalize circumambulation in 1-dehydrobenzene anions.^{12,13} Ben-Ari et al. have reviewed the chemistry of the 1,2-hydrogen shift isomers of several aryl cations and aryl anions.¹⁴ They reported that most hydrogen shift isomers are kinetically stable with high energetic barriers to unimolecular isomerization in the gas phase. In this study, we discuss a more facile “ring walking”

Scheme 1. Products from Collision-Induced Dissociation of the *ortho*-, *meta*-, and *para*-Methoxybenzoate Anions



mechanism with a lower energy barrier to rationalize gas phase dissociation of methoxyphenyl anions. The ion fragmentation

Scheme 2. Proposed Mechanism for the Loss of Formaldehyde from the 1-Dehydro-2-methoxybenzene Anion (7) Produced by Decarboxylation of *ortho*-Methoxybenzoate Anion (4)



tenets concluded from this investigation are diagnostically useful for structure elucidation of methoxybenzoic acid congeners.¹⁵

RESULTS AND DISCUSSION

A comparison of CID spectra recorded from the m/z 151 anions generated from *ortho*- (4), *meta*- (5), and *para*-methoxybenzoic acid (6) indicated that all three isomers initially underwent a facile expulsion of a CO_2 molecule to produce ions of m/z 107 (Figure 1a,c,e). However, the spectrum recorded from the *ortho* isomer was distinctly different from those of the *meta* and *para* isomers. For example, the product ion spectrum of the *ortho*-methoxybenzoate anion showed an additional peak at m/z 77, which indicated that this compound underwent a fragmentation mechanism specific to the *ortho* isomer (Figure 1a). To investigate this phenomenon further, we mass selected the hydrogen-shift isomeric anions¹² produced by decarboxylation of the *ortho*, *meta*, and *para* precursors and subjected them to collision-induced dissociation (Figure 1b,d,f). The results showed that only the spectrum of the anion 7 generated from the *ortho* isomer showed a peak at m/z 77 for a loss of a 30 Da neutral molecule (Figure 1b). We envisaged that this loss of a 30 Da neutral molecule represents an elimination of a formaldehyde molecule by an *ortho*-isomer-specific fragmentation mechanism. In contrast, the spectra of *meta*- and *para*-isomers did not show a

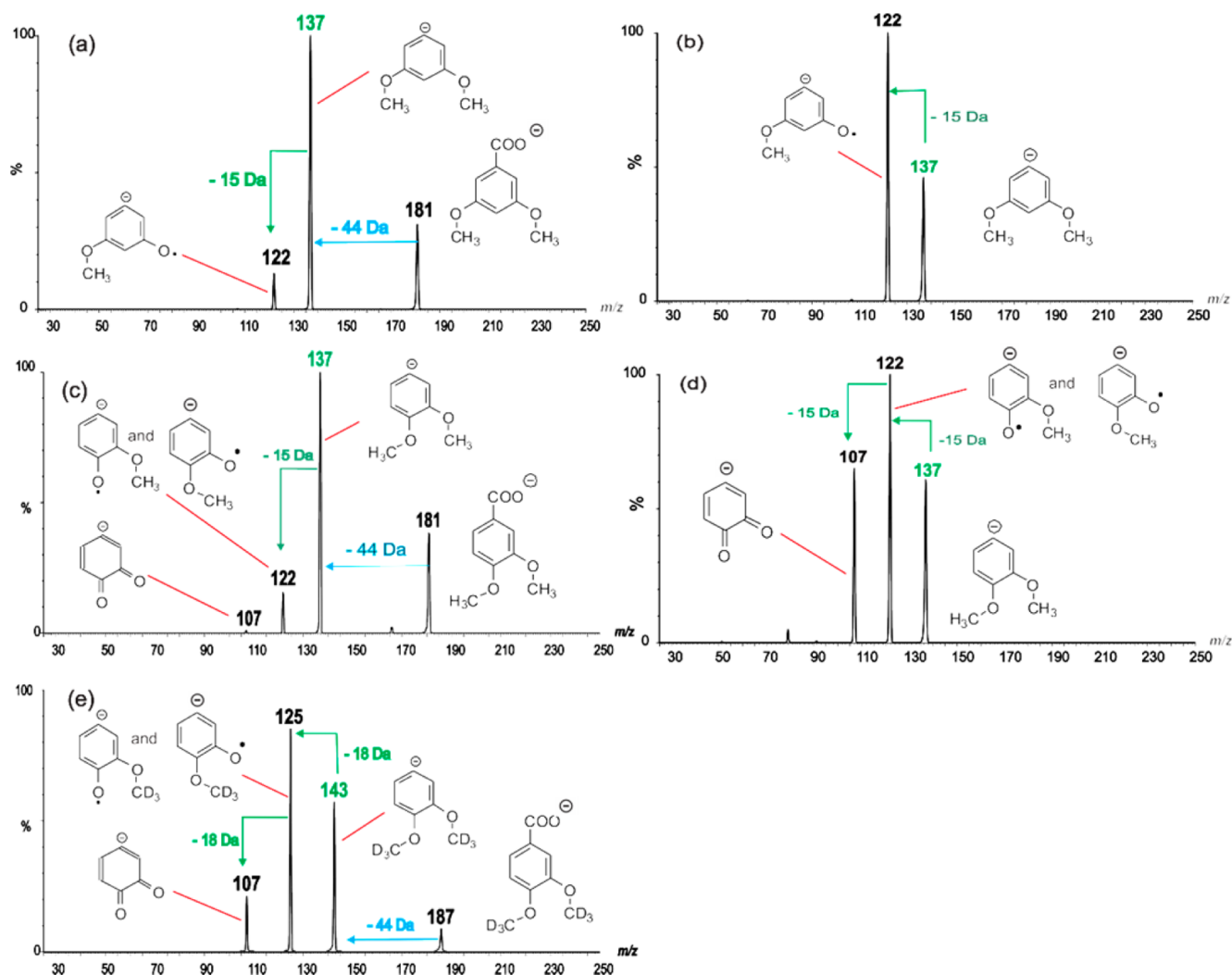


Figure 2. Unit-resolution CID mass spectra recorded from the m/z 181 anion generated from (a) 3,5- and (c) 3,4-dimethoxybenzoic acid, and (e) that of the m/z 187 anion generated from 3,4- $[\text{C}^2\text{H}_3]$ dimethoxybenzoic acid. The product ion spectra (b and d) were recorded from in-source-generated m/z 137 ions from 3,5-, and 3,4-dimethoxybenzoic acid, respectively (all spectra were recorded at 20 eV, except the one shown in panel e, which was recorded at a higher collision energy setting).

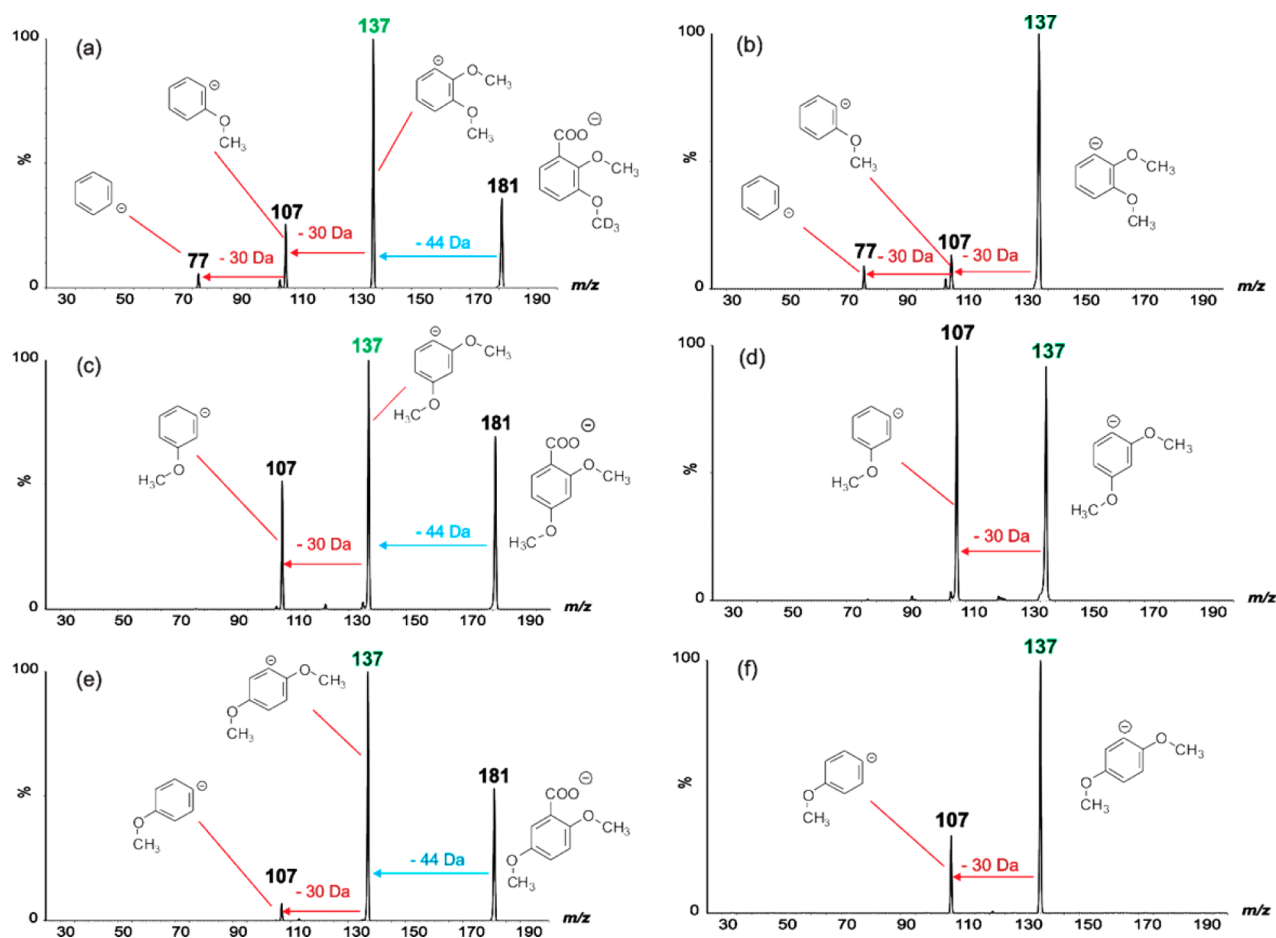


Figure 3. Unit-resolution CID mass spectra, recorded at a collision energy setting of 20 eV, from the m/z 181 anion generated from (a) 2,3-, (c) 2,4-, and (e) 2,5-dimethoxybenzoic acid, and (b, d, and f) those of their respective in-source-generated m/z 137 ions. Note: the smaller m/z 137 ion undergoes more fragmentation at 20 eV than the larger m/z 181 ion.

peak at m/z 77 for a formaldehyde loss; instead, peaks were observed at m/z 92 for methyl radical losses (Scheme 1).

Subsequent experiments confirmed that the positional integrity of the constituent atoms in the m/z 107 product ions remain unaffected within the time duration of the tandem mass spectrometric fragmentations conducted inside a collision cell of a tandem-quadrupole instrument. In other words, the hydrogen-shift isomers 7, 8, and 9 do not undergo isomerization to a stable common structure. This is noteworthy because, for example, isomeric $C_7H_7O^-$ ions generated from anisole have been reported to undergo major interconversions upon collisional activation.¹⁶ Hydrogen scrambling in positively charged aromatic systems and protonated arenes, particularly by 1,2-hydride transfer mechanisms, is a widely studied phenomenon.¹⁷ Fragmentation experiments^{18–21} and quantum mechanical calculations for negative ions have shown that the energy barriers for proton-shift isomerization are exceedingly high.¹⁴ Nevertheless, 1,2-proton transfers have been suggested to sometimes occur in phenyl anions.^{13,22}

From our results, it was clear that a methoxy group should be present at the ring position ortho to the negative charge-bearing carbon atom in order to eliminate a formaldehyde molecule because neither anion 8 nor 9 underwent a formaldehyde loss. This is a diagnostically useful generalization because many methoxy-substituted aromatic carboxylic acids are found as natural products (Structures 1–3) and synthetic intermediates. A mechanism analogous to a pathway that had been previously

proposed for the loss of an aldehyde molecule from anions generated from *O*-alkyl ethers of *ortho*-hydroxybenzoic acids may be postulated to rationalize this ortho-specific elimination of formaldehyde.⁵ The carbanion-mediated two-step mechanism proposed here resembles the E1cB mechanism known in organic chemistry.²³ After the initial decarboxylation, the *o*-methoxyphenyl anion that is formed (7) undergoes an internal proton transfer from the methyl group to give the intermediate 13. A charge-mediated β -scission of the Ph—O bond of anion 13 then forms a phenyl anion (m/z 77) and eliminates a formaldehyde molecule (Scheme 2).

To establish a general tenet that can be used for structure elucidation, we conducted further experimentation with the six isomeric dimethoxybenzoic acids. The results revealed that only certain specific anions produced by the initial decarboxylation fail to undergo the formaldehyde loss. For example, neither the spectrum of 3,5-dimethoxybenzoate anion nor that of its decarboxylated product shows a peak for a 30 Da formaldehyde loss (Figure 2a,b). This was predicted in our generalization because 3,5-dimethoxybenzoate does not bear a methoxy group on the ring carbon adjacent to the carboxyl group. Instead, the 3,5-dimethoxyphenyl anion lost a methyl radical to show a peak m/z 122 by a fragmentation mechanism analogous to that proposed for *meta*- and *para*-methoxyphenyl anions (Figure 2a,b).

The spectrum 3,4-dimethoxybenzoate anion, on the other hand, showed a small peak at m/z 107 (Figure 2c). The peak at

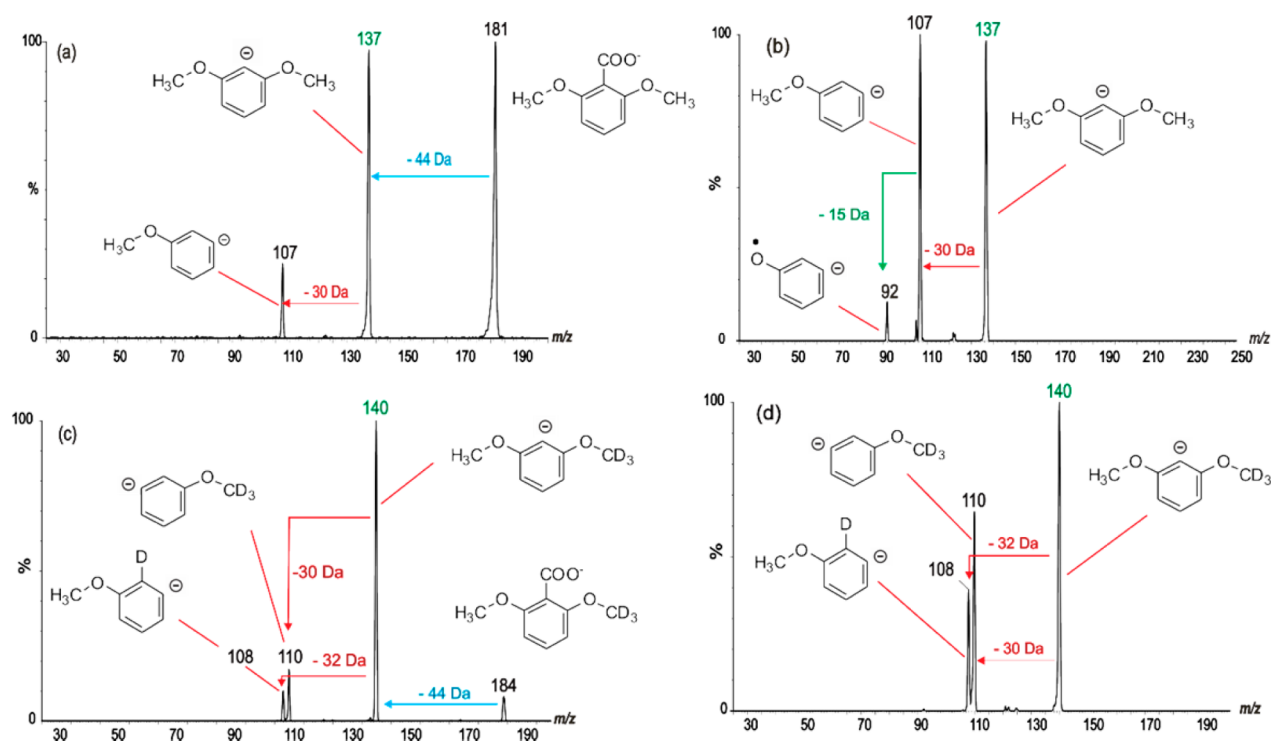


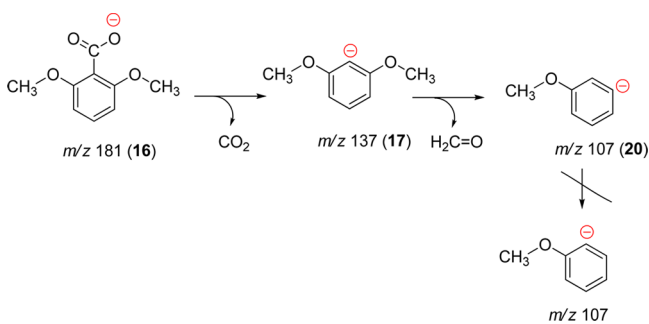
Figure 4. Unit-resolution CID mass spectra, recorded at a collision energy setting of 20 eV, from the m/z 181 anion generated from (a) 2,6-dimethoxybenzoic acid and (c) the m/z 184 ion from 2-methoxy-6- $[C^2H_3]$ methoxy benzoic acid (15), and (b and d) those of their respective in-source-generated m/z 137 and 140 ions. Note: spectra of 2,6-dimethoxybenzoic acid were recorded at 20 eV, and those of 2-methoxy-6- $[C^2H_3]$ methoxy benzoic acid were recorded at a higher collision energy setting.

m/z 107 in the product ion spectrum of the m/z 137 ion, which was generated in the ion source from 3,4-dimethoxybenzoate anion, appeared to indicate a loss of a 30 Da unit from the precursor ion (Figure 2d). At a first look, the 3,4-dimethoxybenzoate anion seemed to violate our generalization about formaldehyde loss because the 1-dehydro-3,4-dimethoxybenzene anion does not bear a methoxy group adjacent to the charge-bearing carbon. The product ion spectrum recorded from the m/z 137 ion showed two intense peaks at m/z 122 and 107 (Figure 2d). However, we could subsequently demonstrate that the m/z 107 peak represents two consecutive methyl radical losses (Figure 2d) by a homolytic fragmentation process that blatantly violates the so-called EE rule advocated by some spectrometry textbooks.²⁴ On the other hand, many violations of this rule have been documented.^{24–29} The formation of an m/z 107 ion from a 3,4-dimethoxybenzoate anion can be attributed to a formation of an *ortho*-quinone anion and not to a formaldehyde loss from the m/z 137 (Figure 2d). To confirm that the m/z 107 ion from 3,4-dimethoxybenzoate is not due to a formaldehyde loss, we synthesized 3,4-di- $[C^2H_3]$ methoxybenzoic acid (14) and recorded its CID spectrum. In fact, the m/z 187 ion generated from acid 14 initially lost CO_2 to produce an m/z 143 ion, which then underwent two consecutive CD_3 radical losses (and not a $[^2H_2]$ formaldehyde loss) to produce the ion for m/z 107 (Figure 2e). Thus, the formation of an m/z 107 ion, which is not due to a formaldehyde loss, suggested that the 1,2-relationship of the two methoxy groups can be established by this charge-remote two-step radical loss. For example, the spectrum of the 3,5-dimethoxybenzoate anion shows a peak only for one methyl radical loss, although it bears two methoxy groups because the methoxy groups are not adjacent to each other (Figure 2a). In contrast, the spectrum of the 3,4-dimethoxy-

benzoate anion shows a peak for two methyl radical losses because the methoxy groups are adjacent to each other (Figure 2d).

The spectrum of 2,3-dimethoxybenzoic acid, a compound with two methoxy groups adjacent to the carboxyl group, showed two peaks at m/z 107 and 77 for two consecutive formaldehyde losses (Figure 3a,b). In contrast, the spectra of 2,4- and 2,5-dimethoxybenzoic acids showed only one peak for a formaldehyde loss, confirming that only the methoxy group adjacent to the $COOH$ group participates specifically in the elimination (Figure 3c–f). The unanticipated finding was that the m/z 137 ion generated from 2,6-dimethoxybenzoic acid underwent only one formaldehyde loss although the compound bears two methoxy groups on both sides of the carboxylate group (Figure 4a,b). This observation provided unequivocal evidence to conclude that the negative charge located on a phenyl ring does not “ring walk” by a 1,2-proton shift mechanism. Our results are congruent with Ben-Ari et al.’s observations on hydrogen-shift isomers of 2-, 3-, and 4-dehydrobenzenesulfonates.¹⁴ They reported that the energies of the transition states involved for the hydrogen migration are much higher than those of the other competing pathways.¹⁴ The peak observed at m/z 107 in the spectrum of the 1-dehydro-2,6-dimethoxybenzene anion, formed upon activation of the 2,6-dimethoxybenzoate anion, confirmed that it undergoes an elimination of formaldehyde (Figure 4a; Scheme 3). In the anion formed in this way (1-dehydro-3-methoxybenzene anion 20), the charge is specifically located on the carbon atom meta to the methoxy group, thereby preventing a second formaldehyde elimination. In other words, the negative charge does not “ring walk” if the methoxy group is not located at an adjacent carbon. To confirm the elimination mechanism, we synthesized the deuteriated analogue, 2-methoxy-6- $[C^2H_3]$ methoxy benzoic acid (15) and recorded its mass spectrum. Figure 4c,d illustrates that

Scheme 3. Gas-Phase Fragmentation of 2,6-Dimethoxybenzoate Anion



the anion generated by the initial decarboxylation eliminates either a $\text{H}_2\text{C}=\text{O}$ or a $\text{D}_2\text{C}=\text{O}$ molecule to generate the m/z 110 or 108 ions, respectively.

To determine the relative energies associated with the dissociative steps of 2,6-dimethoxy benzoate (16), a series of QM computations were carried out using the B3LYP density functional and the 6-311++G(d,p) basis set. The results are summarized in Figure 5. In the first step, a molecule of CO_2 is eliminated in a barrierless step to form the 1-dehydro-2,6-dimethoxybenzene anion (m/z 137; 17) as an intermediate. The calculated relative energy of intermediate 17 formed by the CO_2 elimination is about 35.3 kcal/mol above that of the starting carboxylate anion 16. Intermediate 17 then twists into a more stable intermediate (18) via the transition state TS17–18. Intermediate 18 then transfers a proton to the charge center on the ring via 5-membered transition state TS18–19. The energy of the transition state TS18–19 lies about 19.6 kcal/mol above

that of the starting intermediate anion 18. Intermediate 19 formed in this way, then eliminated a formaldehyde molecule via the transition state TS19–20 to generate the 1-dehydro-3-methoxybenzene anion (m/z 107; 20). We also evaluated energetics associated with other alternative procedures, including a possible concerted cyclic E2 mechanism. However, a transition state to support a concerted mechanism could not be located. Instead, we consistently found two transition states that were associated with the two-step process of eliminating formaldehyde.

In the spectrum of 2-methoxy-6- $[\text{C}^2\text{H}_3]$ methoxybenzene anion (Figure 4c), the intensity of the m/z 108 peak was significantly lower than that at m/z 110, which indicated a kinetic isotope effect (KIE) of the magnitude 1.67. Figure 6 and Table 1 show the optimized structures and KIE values calculated by QM computations of dissociation products of 18a and 18b, which are two conformers of 1-dehydro-2-methoxy-6- $[\text{C}^2\text{H}_3]$ methoxybenzene. The Gibbs free energies for a transition state (G^\ddagger) and for a reactant (G) were calculated as described in the Computational Methods section. The ΔG^\ddagger is equal to the difference between G^\ddagger and G converted to kilocalorie per mole (kcal/mol) units. KIE was calculated as the ratio of two rate constants $k_{\text{H}}/k_{\text{D}}$ for protonated and deuterated reactants by the procedure described by Zeller and Strassner.^{30,31} Calculated KIE values ($k_{\text{H}}/k_{\text{D}}$) by QM computations for ion dissociative steps 18 \rightarrow TS18–19 and 19 \rightarrow TS19–20 were 6.6 and 1.3, respectively (Figure 6; Table 1). Despite high margins of error, a KIE value as large as 2.0–4.0 or greater is considered to demonstrate the participation of a cleavage of a C–H/D bond in the rate-determining step.³² Our experimental value of 1.67 (Figure 4d) indicates only a secondary isotope effect, which suggests that in

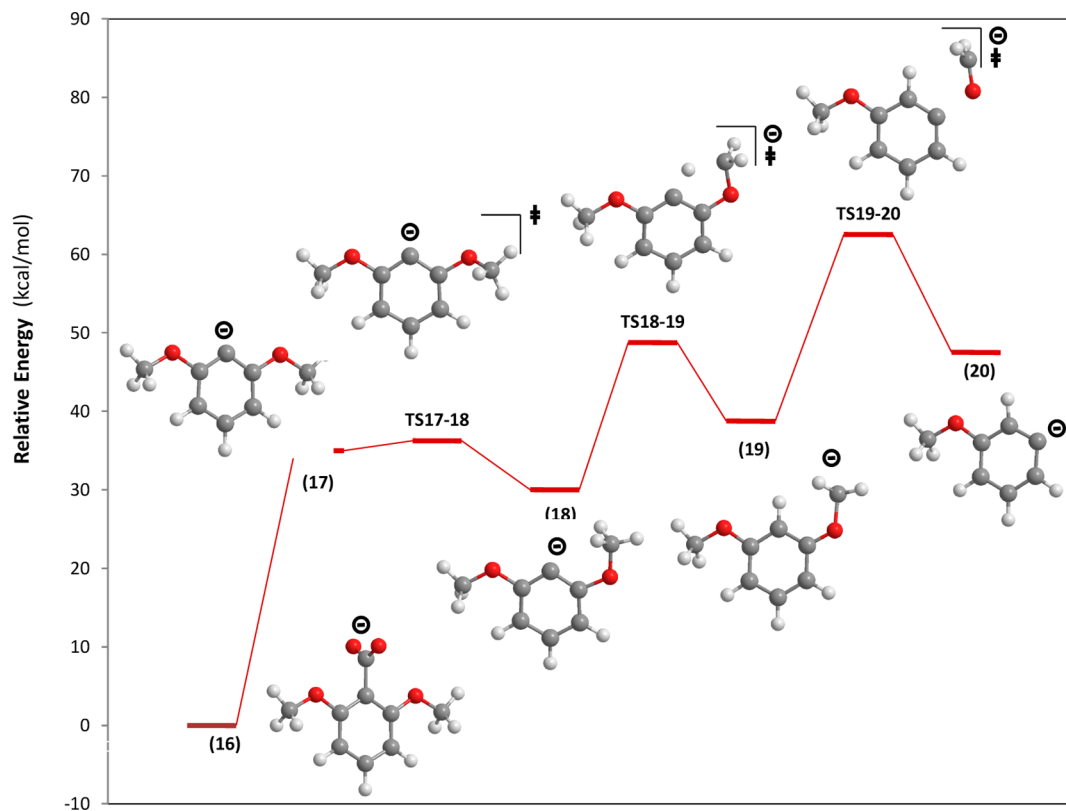


Figure 5. Relative energies (in kcal/mol) and structures of energy-optimized product ions and transition states associated with the dissociation of 2,6-dimethoxybenzoate anion (16).

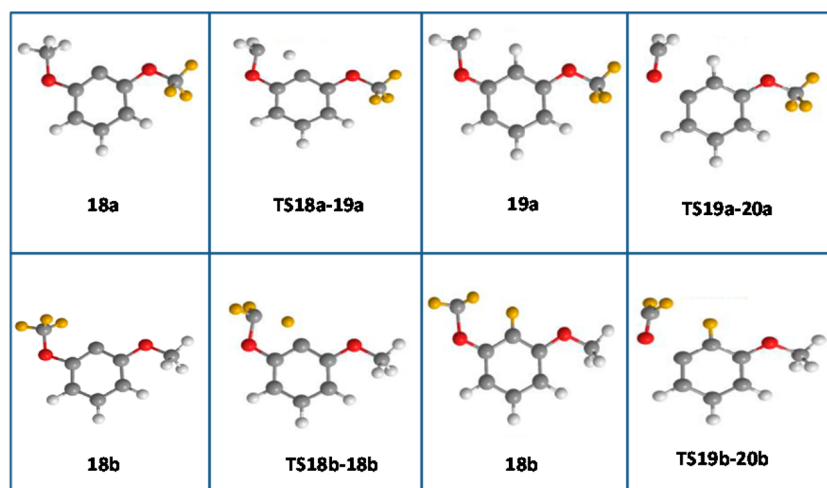


Figure 6. Energy-optimized species of dissociation products of **18a** and **18b**, two conformers of 1-dehydro-2-methoxy-6- $[\text{C}^2\text{H}_3]$ methoxybenzene anion (yellow-colored atoms represent deuterium).

Table 1. KIE Values ($k_{\text{H}}/k_{\text{D}}$) Calculated by QM Computations for the Two Ion Dissociative Steps $18 \rightarrow \text{TS}18-19$ and $19 \rightarrow \text{TS}19-20$ for Two Conformers of 1-Dehydro-2-methoxy-6- $[\text{C}^2\text{H}_3]$ methoxybenzene (**18a** and **18b**) and the Two Intermediate Products (**19a** and **19b**), Respectively

dissociative step	G (hartrees)	G^\ddagger (hartrees)	ΔG^\ddagger (kcal/mol)	k (s^{-1})	$t_{1/2}$ (s^{-1})	$k_{\text{H}}/k_{\text{D}}$
18a \rightarrow TS18a-19a	-460.702 389	-460.670 482	20.0	1.31×10^{-2}	52.8	6.6
18b \rightarrow TS18b-19b	-460.702 409	-460.668 727	21.1	2.00×10^{-3}	346.0	
19a \rightarrow TS19a-20a	-460.687 501	-460.649 093	24.1	1.34×10^{-5}	51611.2	1.3
19b \rightarrow TS19b-20b	-460.686 909	-460.648 256	24.3	1.04×10^{-5}	66900.5	

the rate-determining step (the $\text{H}_2\text{C}=\text{O}$ elimination from **19**), a direct cleavage of a C–H bond is not involved. This agrees well with the computational prediction that the energy barrier between **18** and **19** (the C–H bond cleavage via **TS18–19**) is lower than that between **19** and **20** (formaldehyde elimination via **TS19–20**). Presumably, more accurate estimates for the free energy of activation may be calculated by advanced methods; however, the procedure we used here is widely accepted as the general method for interpreting experimentally determined KIEs and eventually relating the calculated values to proposed reaction mechanisms.³¹

Furthermore, our results from the 1-dehydro-2,6-dimethoxybenzene **17**, and 2-methoxy-6- $[\text{C}^2\text{H}_3]$ methoxybenzene anions showed that the formaldehyde elimination follows a specific pathway without any indication of a loss of integrity due to scrambling. In a previous report, however, Kleingeld and Nibbering³³ concluded that there is an equilibrium between the three deuterium atoms on the methoxy group and the *ortho*-aryl hydrogens prior to the loss of formaldehyde during fragmentation of the 1-dehydro-2- $[\text{C}^2\text{H}_3]$ methoxybenzene anion (m/z 110). Apparently, the m/z 110 ion, isolated in an FT-ICR cell, showed peaks for two nearly equal losses of CD_2O (32 Da) or CDHO (31 Da).³³ In contrast, as mentioned above, our results were obtained on a tandem quadrupole instrument, and upon activation, the 2-methoxy-6- $[\text{C}^2\text{H}_3]$ methoxybenzene anion showed peaks only for a loss of CD_2O (32 Da) or CH_2O (30 Da) (Figure 4d). Clearly, the overall fragmentation processes that the 1-dehydro-2- $[\text{C}^2\text{H}_3]$ methoxybenzene anions undergo are different in the two instruments. In an FT-ICR instrument (and other ion-trapping instruments), mass-isolated ions are activated for longer periods of time than in tandem quadrupole instruments. Moreover, isolated ions in ion-trapping instruments, particularly in quadrupolar ion traps, are prone to additional ion/molecule

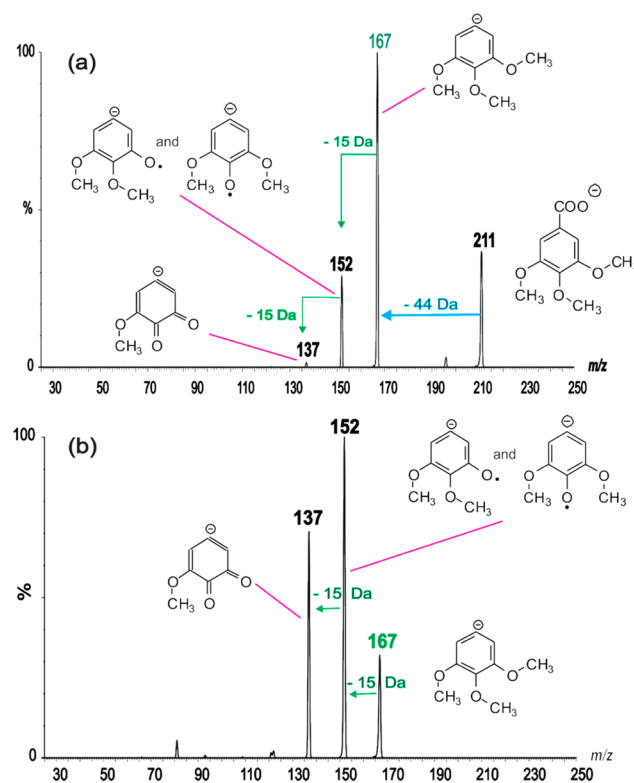


Figure 7. Unit-resolution CID mass spectra recorded for 3,4,5-trimethoxybenzoic acid generated from (a) the m/z 211 anion and (b) its in-source-generated m/z 167 ion.

reactions with residual molecules such as water.³⁴ Evidently, the integrity of the 1-dehydromethoxybenzene anions are not lost

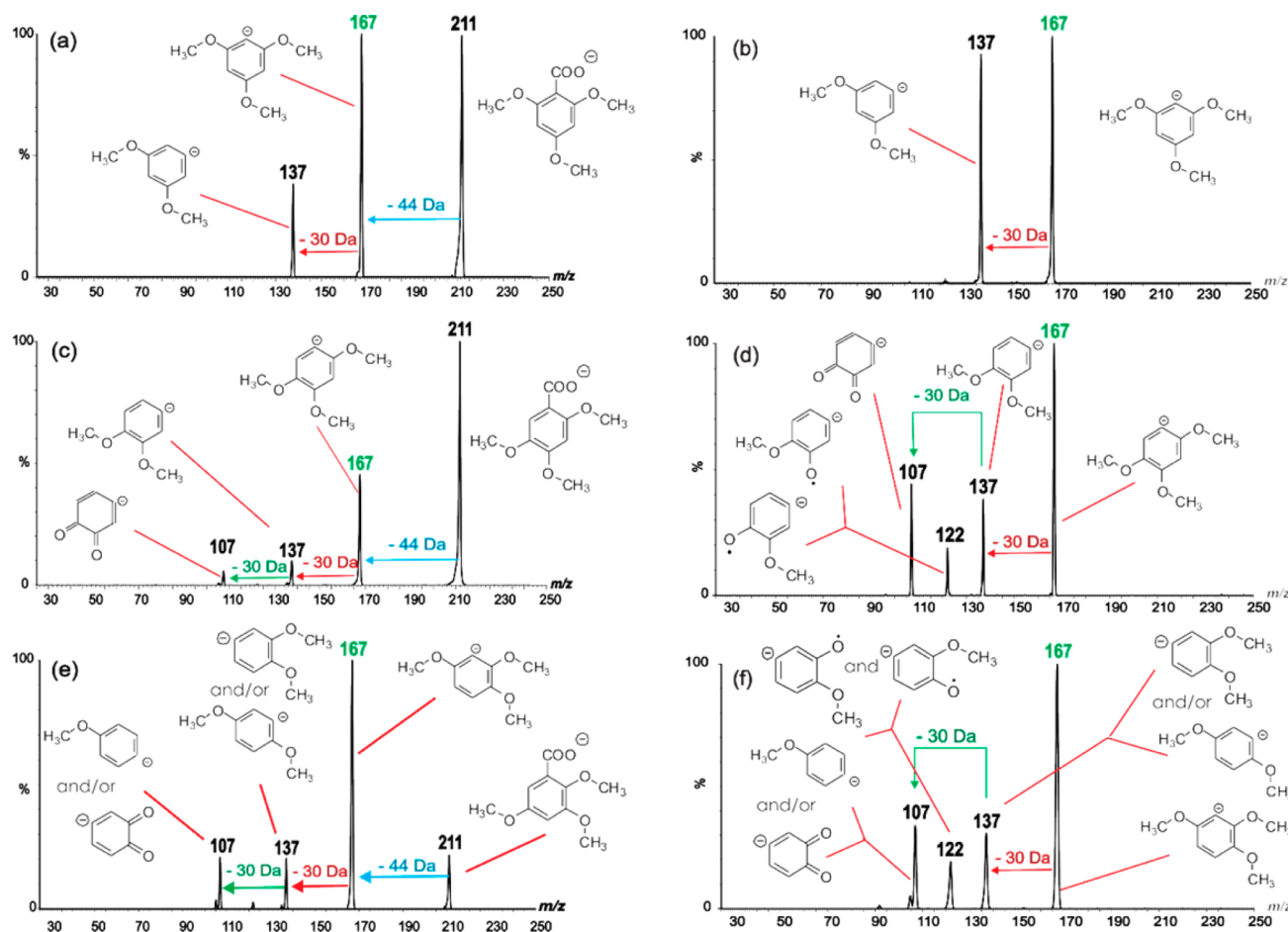
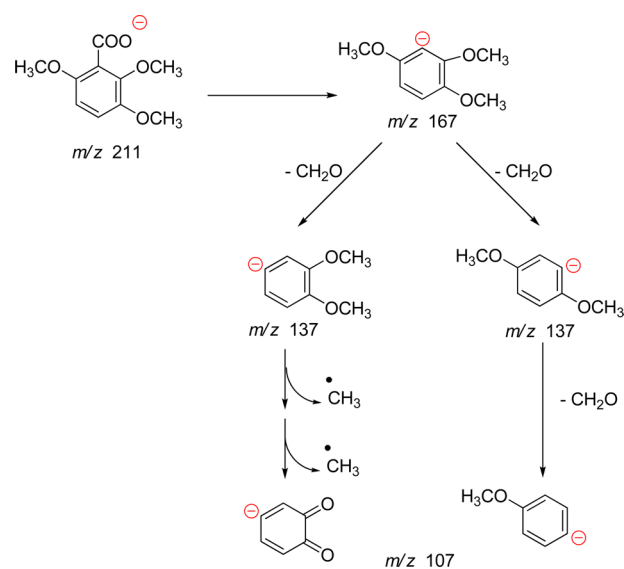


Figure 8. Unit-resolution CID mass spectra recorded from the m/z 211 anion generated from (a) 2,4,6-, (c) 2,4,5-, and (e) 2,3,6-trimethoxybenzoic acid, and (b, d, and f) those of their respective in-source-generated m/z 167 ions.

during the brief activation period in tandem quadrupole instruments. Moreover, at a first look, the calculated rate-limiting rate constants may appear to be too large for a formaldehyde loss during the short ion residence time in the collision cell. However, once the precursor ion is activated in the collision cell, it undergoes a rapid loss of formaldehyde within the dwell time in the collision cell (Table 1). If collision energy is not applied, then the ion does not eliminate formaldehyde during its residence time in the cell.

The spectra recorded from trimethoxybenzoic acids provided further validation that our generalizations are applicable to many other examples. The spectrum of 3,4,5-trimethoxybenzoate showed a peak at m/z 167 for a CO_2 loss followed by peaks at m/z 152 and 137 for two consecutive methyl radical losses to form the predicted orthoquinone anion (Figure 7a). In contrast, 1-dehydro-2,4,6-trimethoxybenzene anion generated from 2,4,6-trimethoxybenzoate underwent only one formaldehyde loss (Figure 8a,b). The 1-dehydro-2,4,5-trimethoxybenzene anion generated from 2,4,5-trimethoxybenzoate, on the other hand, showed a peak at m/z 137 for a formaldehyde loss, followed by peaks at m/z 122 and 107 for two consecutive methyl radical losses (Figure 8c,d). The spectrum of 1-dehydro-2,3,6-trimethoxybenzene anion generated from 2,3,6-trimethoxybenzoic acid, with two methoxy groups adjacent to the carboxyl group, showed a peak at m/z 137 for an initial formaldehyde loss. The ion of nominal mass m/z 107 is a composite because it can originate from a second formaldehyde loss or from two successive methyl radical losses (Figure 8e,f; Scheme 4).

Scheme 4. Gas-Phase Fragmentation of 2,3,6-Trimethoxybenzoate Anion



The fragmentation of 2,3,4-trimethoxybenzoate ion generated by deprotonation is the most interesting case. As we envisaged, the 1-dehydro-2,3,4-trimethoxybenzene anion (m/z 167) formed by decarboxylation underwent three consecutive formaldehyde losses and produced ions for peaks observed at m/z

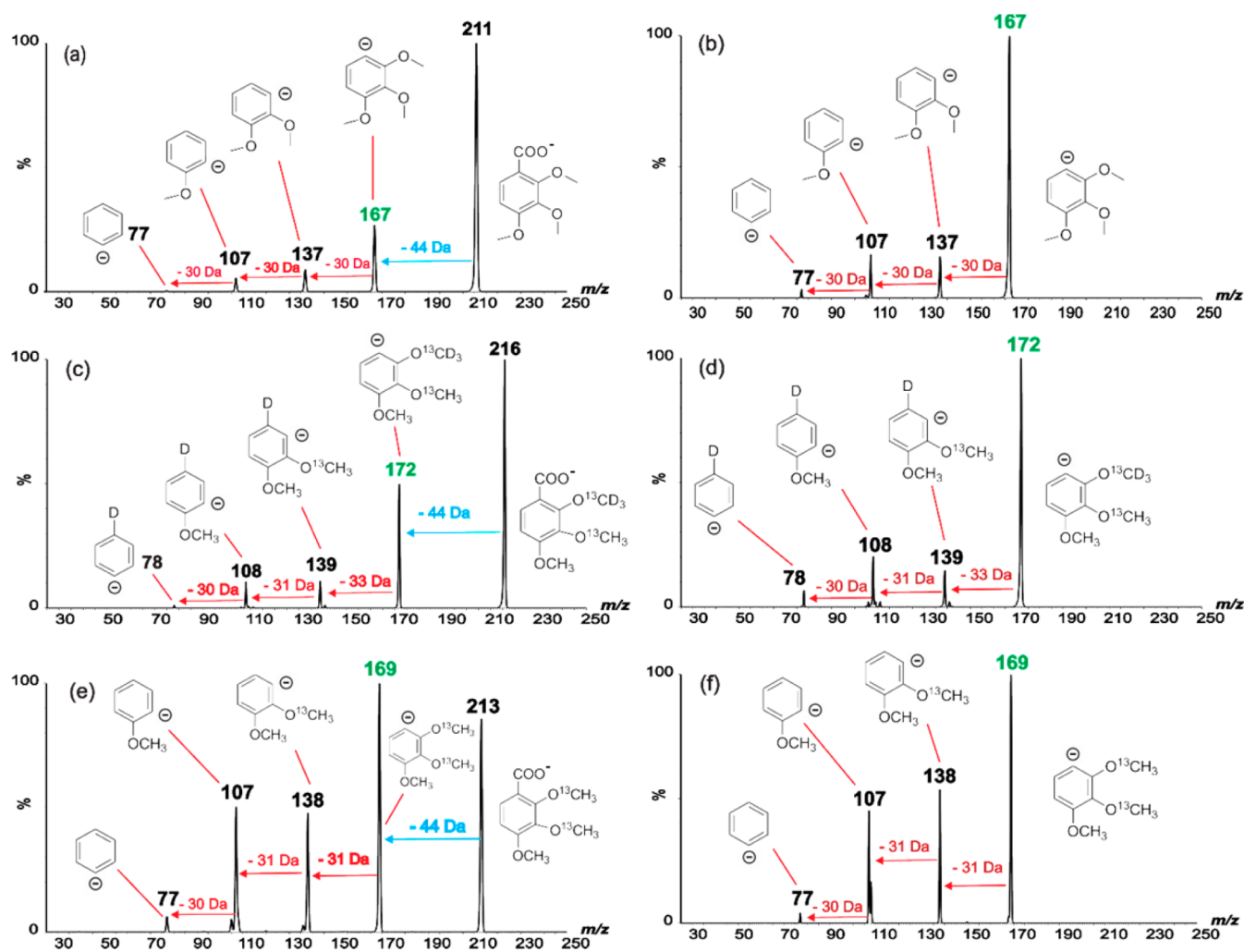


Figure 9. Unit-resolution CID mass spectra recorded from the m/z 211 anion generated from (a) 2,3,4-trimethoxybenzoic acid, (c) m/z 216 anion generated from 2- $^{13}\text{C}_2\text{H}_3$ methoxy-3- ^{13}C methoxy-4-methoxybenzoic acid (21), and (e) m/z 213 anion generated from 2,3-di- ^{13}C methoxy-4-methoxybenzoic acid, and (b, d, and f) those of their respective in-source-generated m/z 167, 172, and 169 ions.

137, 107, and 77 (Figure 9a,b; Scheme 5). To confirm the circumambulatory movement of the ring charge, we synthesized 2- $^{13}\text{C}_2\text{H}_3$ methoxy-3- ^{13}C methoxy-4-methoxybenzoic acid (21). The spectrum shows a peak at m/z 139 for the loss of the initial 33 Da molecule ($^2\text{H}_2^{13}\text{C}=\text{O}$). The m/z 139 ion then lost a 31 Da molecule ($\text{H}_2^{13}\text{C}=\text{O}$), followed by an elimination of 30 Da molecule ($\text{H}_2\text{C}=\text{O}$) (Figure 9b,c). Analogously, the spectrum of 2,3- ^{13}C dimethoxy-4-methoxybenzoic acid (22) showed peaks at m/z 138, 107, and 77 for three consecutive losses of $\text{H}_2^{13}\text{C}_1=\text{O}$, $\text{H}_2^{13}\text{C}=\text{O}$, and H_2CO , respectively (Figure 9e,f).

CONCLUSIONS

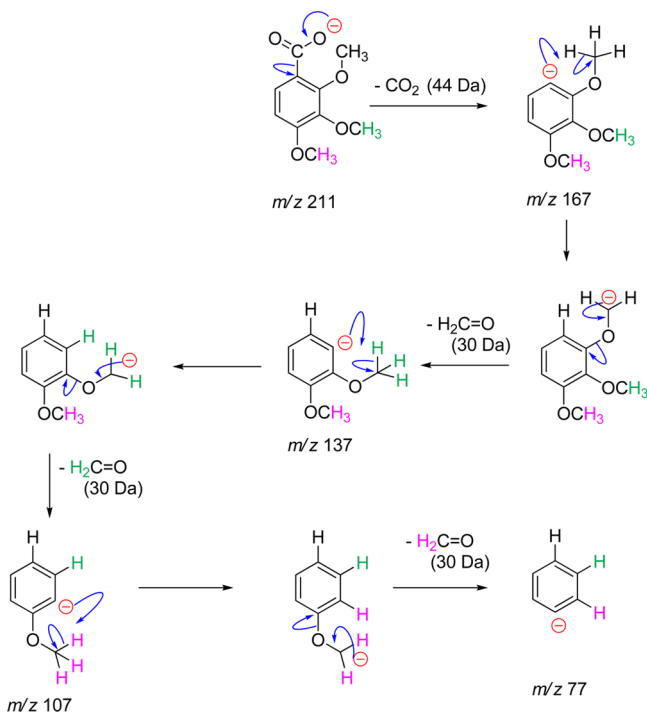
Upon activation in the collision cell of a tandem mass spectrometer, a negative charge located on a ring carbon atom of a phenyl group does not easily undergo scrambling by a 1,2-proton-shift to lose the positional integrity of ring protons. However, if a methoxy group is attached to the ring carbon atom adjacent to the charge site, then the charge migrates to the adjacent position by losing a formaldehyde molecule by a stepwise process. For example, a proton transfer from the methoxy group of the 1-dehydro-2-methoxybenzene anion to the charge site generates a “hydrogen-shift” isomer as an intermediate,

which then loses formaldehyde to form a phenyl anion. If additional methoxy groups were available on adjacent positions, then the negative charge circumambulates by successive formaldehyde eliminations. In contrast, 1-dehydro-3-methoxybenzene and 1-dehydro-4-methoxybenzene anions do not eliminate formaldehyde but lose a methyl radical by homolytic cleavage.

EXPERIMENTAL SECTION

Materials and Methods. All chemicals were used as purchased from commercial suppliers. Reactions were monitored by thin layer chromatography. Purification of synthetic sample was performed by flash chromatography on silica gel (particle size 60 μm). Structures of all synthetic products were confirmed by ^1H NMR, ^{13}C NMR, and mass spectrometry. NMR spectra were recorded on a 500 MHz spectrometer (500 MHz for ^1H and 125 MHz for ^{13}C acquisitions). Chemical shifts (δ) are reported in parts per million with tetramethylsilane or the solvent resonance as the internal standard. Coupling constants (J) are given in hertz. Multiplicities are classified as follows: s, singlet; d, doublet; t, triplet; q, quartet; sept, septet; combinations thereof; m, multiplet; or br, broad signal. Two-dimensional NMR methods (HSQC, HMBC) were used for the assignment. EI mass spectra (70 eV) were recorded by GC-MS. Collision-induced dissociation (CID) mass spectra were recorded on a triple-quadrupole tandem mass spectrometer equipped with a Z-spray electrospray ion source. Samples were infused as acetonitrile–water– NH_3 (1:1:2 $\times 10^{-3}$) solutions at a flow

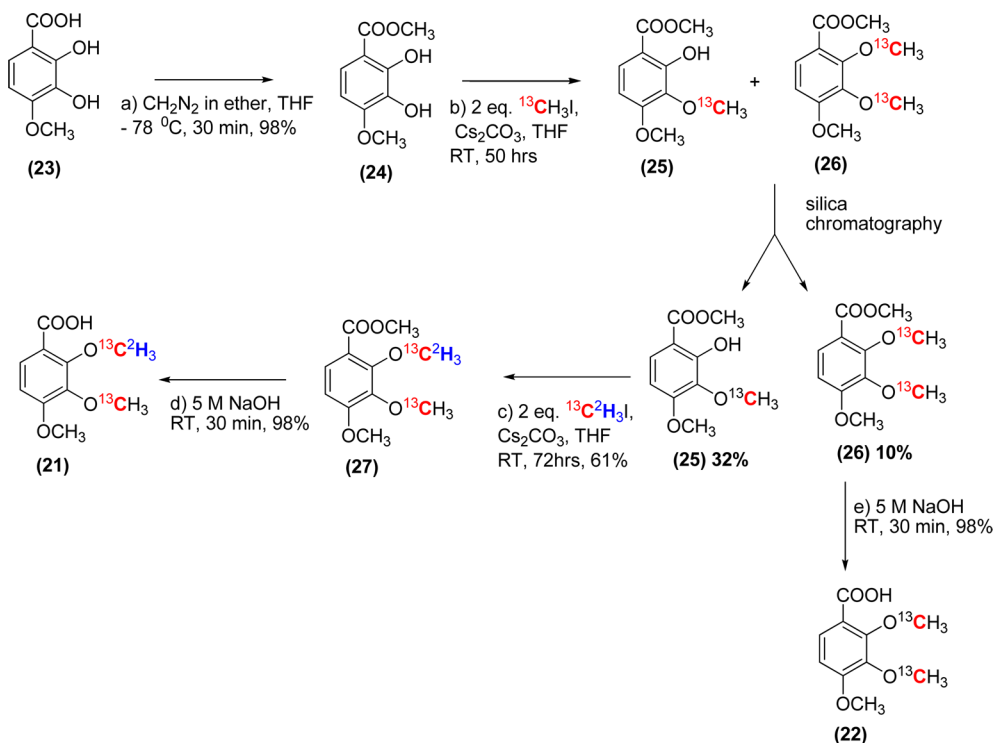
Scheme 5. Consecutive Losses of Three Formaldehyde Units from the 2,3,4-Trimethoxyphenyl Anion Produced by Decarboxylation of 2,3,4-Trimethoxybenzoate Anion



rate of 10 $\mu\text{L}/\text{min}$. Source and the desolvation temperatures were held at 70 and 200 $^{\circ}\text{C}$, respectively. Argon gas pressure in the collision cell was set to attenuate the precursor ion transmission by 30–50%.

Synthesis of 2- $^{13}\text{C}^2\text{H}_3$]Methoxy-3- ^{13}C]methoxy-4-methoxybenzoic Acid (21) and 2,3- ^{13}C]Dimethoxy-4-methoxybenzoic Acid (22)

Scheme 6. Synthesis of 2- $^{13}\text{C}^2\text{H}_3$]Methoxy-3- ^{13}C]methoxy-4-methoxybenzoic Acid (21) and 2,3- ^{13}C]Dimethoxy-4-methoxybenzoic Acid (22)

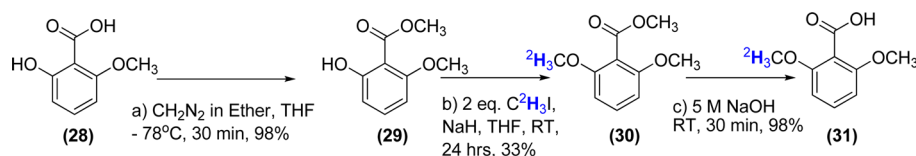


Acid (22). Compounds 21 and 22 were synthesized by the procedure summarized in Scheme 6.

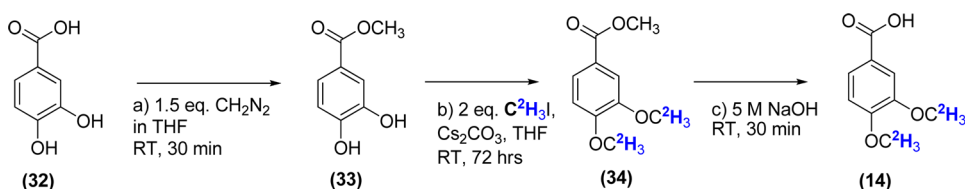
Methyl 2,3-Dihydroxy-4-methoxybenzoate (24). An ethereal solution of diazomethane (3 mL, ~ 250 mM) was added to a solution of 2,3-dihydroxy-4-methoxy benzoic acid (23, 95 mg, 0.5 mmol) in THF (2 mL) at -78 $^{\circ}\text{C}$. The mixture was stirred for 30 min at -78 $^{\circ}\text{C}$ and quenched with acetic acid (50 μL). The solvent was evaporated to yield 24 as a white solid (100 mg, 98%). ^1H NMR (500 MHz, CD_3OD) δH 6.59 (1H, d, $J = 9.0$, H-5), 7.39 (1H, d, $J = 9.0$, H-6), 3.89 (3H, s, 4-OCH₃), 3.90 (3H, s, COOCH₃); ^{13}C NMR (125 MHz, CD_3OD) δc 172.0 (COO), 52.5 (COOCH₃), 106.0 (C-1), 135.0 (C-2), 135.0 (C-3), 154.0 (C-4), 104.0 (C-5), 122.0 (C-6), 56.6 (4-OCH₃); methyl signal at δc 52.5, δH 3.90 showed three bond HMBC correlations to the carbonyl group at δc 172; EI m/z (%) 198 (M^+ , 58), 167 (24), 166 (77), 148 (67), 137 (32), 120 (100), 109 (10), 95 (37), 66 (8), 53 (29).

Methyl 2-Hydroxy-3- ^{13}C]methoxy-4-methoxybenzoate (25) and Methyl 2,3- ^{13}C]Dimethoxy-4-methoxybenzoate (26). To a mixture of 24 (60 mg, 0.3 mmol) and Cs_2CO_3 (2 equiv) in anhydrous THF (2 mL) at rt under N_2 was added $^{13}\text{C}_3\text{HI}$ (2 equiv), and the mixture was stirred for 50 h. The reaction was quenched with 1 M HCl (5 mL), and the product was extracted into ethyl acetate. The separated ethyl acetate layer was concentrated to afford a solid (95 mg), which was purified by flash chromatography (silica gel, 10% ethyl acetate/hexane containing 1% acetic acid). Then, 5 mL fractions were collected, fractions 33–45 and 50–64 were pooled, and solvent was evaporated to yield a colorless oily material (26, 6.6 mg, 10%) and a white solid (25, 20 mg, 32%), respectively.

Compound 25. ^1H NMR (500 MHz, CD_3OD) δH 6.61 (1H, d, $J = 9.0$, H-5), 7.60 (1H, d, $J = 9.0$, H-6), 3.88 (3H, s, 4-OCH₃), 3.90 (3H, s, COOCH₃), 3.78 (3H, d, $J = 144$ Hz, 3-O $^{13}\text{C}_3\text{H}_3$); ^{13}C NMR (125 MHz, CD_3OD) δc 171.8 (COO), 52.8 (COOCH₃), 108.8 (C-1), 156.9 (C-2), 137.7 (C-3), 159.7 (C-4), 104.8 (C-5), 127.2 (C-6), 61.0 (3-O $^{13}\text{C}_3\text{H}_3$), 56.7 (4-OCH₃). The positions of the methoxy groups in 25 were confirmed by the strong three-bond HMBC correlations observed from H-5 and H-6 to C-3 and C-2, respectively, and the two-bond HMBC correlation from 3H (3-O $^{13}\text{C}_3\text{H}_3$) to C-3. MS (EI+, m/z (%) 213 (M^+ , 61), 182 (24), 181 (100), 165 (11), 153 (100), 151 (26),

Scheme 7. Synthesis of 2-Methoxy-6-[C²H₃]methoxybenzoic Acid^a

^aReagents and conditions: (a) CH₂N₂ (1.5 equiv), THF, -78 °C, 30 min, 98%; (b) C²H₃I (2 equiv), NaH (2 equiv), THF, rt, 24 h, 30%; (c) 5 M NaOH (0.5 mL), rt, 30 min, 98%.

Scheme 8. Synthesis of 3,4-di[C²H₃]Methoxybenzoic Acid (14)^a

^aReagents and conditions: (a) CH₂N₂ (1.5 equiv), THF, rt, 30 min; (b) C²H₃I (2 equiv), Cs₂CO₃ (2 equiv), THF, rt, 72 h; (c) 5 M NaOH (0.5 mL), rt, 30 min.

137 (51), 123 (24), 122 (16), 121 (31), 120 (36), 109 (25), 95 (21), 94 (23), 66 (25), 53 (33).

Compound 26. ¹H NMR (500 MHz, CD₃OD) δH 6.85 (1H, d, *J* = 9.0, H-5), 7.56 (1H, d, *J* = 9.0, H-6), 3.89 (3H, s, 4-OCH₃), 3.84 (3H, s, COOCH₃), 3.86 (3H, d, *J* = 144 Hz, 2-O¹³CH₃), 3.81 (3H, d, *J* = 144 Hz, 3-O¹³CH₃); ¹³C NMR (125 MHz, CD₃OD) δC 167.7 (COO), 52.4 (COOCH₃), 118.8 (C-1), 155.7 (C-2), 144.2 (C-3), 158.8 (C-4), 108.5 (C-5), 128.0 (C-6), 62.3 (2-O¹³CH₃), 61.3 (3-O¹³CH₃), 56.6 (4-OCH₃); EI *m/z* (%) 228 (M⁺, 91), 212 (10), 197 (100), 196 (72), 181 (13), 180 (39), 166 (15), 153 (33), 137 (20), 109 (12), 94 (17), 66 (21).

Methyl 2-[¹³C²H₃]Methoxy-3-[¹³C]methoxy-4-methoxybenzoate (27). To a stirred solution of methyl 2-hydroxy-3-[¹³C] methoxy-4-methoxybenzoate (25; 18 mg, 0.1 mmol) and 2 equiv of Cs₂CO₃ in anhydrous THF (2 mL) at rt under N₂, was added 2 equiv of ¹³C²H₃I and the mixture was stirred at rt under N₂ for 72 h. The reaction was quenched with 1 M HCl (5 mL), and the product was extracted into ethyl acetate. The organic layer was separated and concentrated. The reaction product was purified by flash-silica chromatography (10% EtOAc/hexane with 1% AcOH) to give a colorless oil (17, 12 mg, 61%).

The structure of compound 27 was confirmed by the strong three-bond HMBC correlations from H-5 and H-6 to C-3 and C-2, respectively, and the two-bond HMBC correlation from 3H (3-O¹³CH₃) to C-3. ¹H NMR (500 MHz, CD₃OD) δH 6.83 (1H, d, *J* = 8.5, H-5), 7.55 (1H, d, *J* = 8.5, H-6), 3.88 (3H, s, 4-OCH₃), 3.83 (3H, s, COOCH₃), 3.80 (3H, d, *J* = 145 Hz, 3-O¹³CH₃); ¹³C NMR (125 MHz, CD₃OD) δC 167.6 (COO), 52.3 (COOCH₃), 118.8 (C-1), 155.7 (C-2), 144.5 (C-3), 158.8 (C-4), 108.5 (C-5), 128.0 (C-6), 61.5 (septet, *J* = 87.5, 2-O¹³C²H₃), 61.4 (3-O¹³CH₃), 56.6 (4-OCH₃); EI *m/z* (%) 231 (M⁺, 100), 215 (12), 200 (100), 182 (20), 153 (28), 137 (20), 109 (12), 53 (10).

2-[¹³C²H₃]Methoxy-3-[¹³C]methoxy-4-methoxybenzoic Acid (21). A solution of 5 M NaOH (0.5 mL) was added to a solution of methyl 2-[¹³C²H₃]methoxy-3-[¹³C]methoxy-4-methoxybenzoate (27; 0.2 mg in 100 μL of methanol), and the mixture was stirred for 30 min at rt. The product was acidified with 1 M HCl and extracted into ethyl acetate. Ethyl acetate was removed under a stream of N₂ to yield 21 as a white solid (0.18 mg, 98%). ¹H NMR (500 MHz, CD₃OD) δH 6.86 (1H, d, *J* = 9, H-5), 7.63 (1H, d, *J* = 9, H-6), 3.89 (3H, s, 4-OCH₃), 3.82 (3H, d, *J* = 145 Hz, 3-O¹³CH₃), and ¹³C NMR (125 MHz, CD₃OD) δC 168.9 (COO), 118.7 (C-1), 155.6 (C-2), 144.2 (C-3), 158.8 (C-4), 108.5 (C-5), 128.3 (C-6), 61.8 (septet, *J* = 87.5, 2-O¹³C²H₃), 61.3 (3-O¹³CH₃), 56.6 (4-OCH₃); EI *m/z* (%) 217 (M⁺, 100), 210 (25), 182 (21), 168 (25), 137 (60), 123 (10), 109 (20), 95 (11), 78 (18), 66 (25), 53 (35).

2,3-[¹³C]Dimethoxy-4-methoxybenzoic Acid (22). A solution of 5 M NaOH (0.5 mL) was added to a solution of 2,3-[¹³C]dimethoxy-4-

methoxybenzoic acid methyl ester (26; 2 mg in 150 μL of methanol), and the mixture was stirred for 30 min at rt. The reaction mixture was acidified with 1 M HCl and extracted into ethyl acetate. Ethyl acetate was removed under a stream of N₂ to yield 1.9 mg (98%) of 22 as a white solid. ¹H NMR (500 MHz, CD₃OD) δH 6.86 (1H, d, *J* = 8.5, H-5), 7.563 (1H, d, *J* = 8.5, H-6), 3.89 (3H, s, 4-OCH₃), 3.90 (3H, d, *J* = 145 Hz, 2-O¹³CH₃), 3.82 (3H, d, *J* = 145 Hz, 3-O¹³CH₃); ¹³C NMR (125 MHz, CD₃OD) δC 168.9 (COO), 118.8 (C-1), 155.6 (C-2), 144.2 (C-3), 158.8 (C-4), 108.6 (C-5), 128.4 (C-6), 62.4 (2-O¹³CH₃), 61.4 (3-O¹³CH₃), 56.6 (4-OCH₃); EI *m/z* (%) 214 (M⁺, 100), 198 (30), 180 (42), 167 (40), 152 (20), 137 (66), 123 (11), 109 (37), 94 (27), 77 (29), 53 (45).

Methyl 2-Methoxy-6-hydroxybenzoate (29). A freshly prepared solution of diazomethane (3 mL, ~250 mM) in ether was added dropwise to a stirred solution of 2-methoxy-6-hydroxybenzoic acid (28; 84 mg, 0.5 mmol) in THF (2 mL) at -78 °C. The mixture was stirred for 30 min at -78 °C and quenched with acetic acid (50 μL). The solvent was evaporated to yield a white solid (29, 88 mg, 97%). ¹H NMR (500 MHz, CD₃OD) δH 6.48 (2H, d, *J* = 8.5, H-3,5), 7.24 (1H, t, *J* = 8.5, H-4), 3.78 (3H, s, 2-OCH₃), 3.85 (3H, s, COOCH₃), and ¹³C NMR (125 MHz, CD₃OD) δC 171.3 (COO), 52.6 (COOCH₃), 108.1 (C-1), 160.9 (C-2), 103.4 (C-3), 134.4 (C-4), 103.4 (C-5), 110.1 (C-6), 56.4 (2-OCH₃); EI *m/z* (%) 182 (M⁺, 34), 150 (100), 136 (8), 122 (45), 107 (85), 93 (7), 79 (10).

Methyl 2-Methoxy-6-[C²H₃]methoxybenzoate (30). To a stirred solution of methyl 2-methoxy-6-hydroxybenzoate (29; 40 mg, 0.22 mmol) and 2 equiv of sodium hydride in 2 mL of anhydrous THF was added 2 equiv of C²H₃I, and the mixture was stirred at rt under N₂ for 24 h. The reaction was quenched with 1 M HCl (5 mL), and the product was extracted into ethyl acetate and concentrated under vacuum. The reaction product was purified by flash silica chromatography (10% EtOAc/hexane with 1% AcOH) to yield a colorless oily material (30) (11 mg, 30%). ¹H NMR (500 MHz, CD₃OD) δH 6.65 (2H, d, *J* = 8.5, 1,5, H-3,5), 7.32 (1H, t, *J* = 8.5, H-4), 3.78 (3H, s, 2-OCH₃), 3.81 (3H, s, COOCH₃); ¹³C NMR (125 MHz, CD₃OD) δC 169.1 (COO), 52.7 (COOCH₃), 114.2 (C-1), 158.7 (C-2), 105.0 (C-3), 132.5 (C-4), 105.0 (C-5), 158.7 (C-6), 56.5 (2-OCH₃); EI *m/z* (%) 199 (M⁺, 35), 168 (100), 153 (12), 107 (22).

2-Methoxy-6-[C²H₃]methoxybenzoic Acid (31). A solution of 5 M NaOH (0.5 mL) was added to a solution of methyl 2-methoxy-6-[C²H₃]methoxy benzoate (30, 2.1 mg) in 300 μL of methanol and was stirred for 30 min at rt. The product was acidified with 1 M HCl and extracted into ethyl acetate. It was concentrated to yield 31 (Scheme 7) as a white solid (1.9 mg, 98%). ¹H NMR (500 MHz, CD₃OD) δH 6.65 (2H, d, *J* = 8.5, H-3,5), 7.31 (1H, t, *J* = 8.5, H-4), 3.81 (3H, s, 2-OCH₃); ¹³C NMR (125 MHz, CD₃OD) δC (125 MHz) 170.1 (COO), 116.5

(C-1), 158.4 (C-2), 105.1 (C-3), 132.2 (C-4), 105.1 (C-5), 158.4 (C-6), 56.4 (2-OCH₃); EI *m/z* (%) 185 (M⁺, 100), 168 (49), 153 (11), 139 (34), 138 (40), 136 (28), 122 (18), 121 (30), 120 (21), 107 (100), 89 (30), 78 (30), 63 (30).

3,4-Di[C²H₃]methoxybenzoic Acid (14). A solution of freshly prepared diazomethane (1.5 equiv) in ether was added dropwise to a stirred solution of 3,4-dihydroxybenzoic acid (32) in 200 μL of THF at -78 °C. The mixture was stirred for 30 min at rt, then solvent was evaporated to yield a white solid residue (33). To a solution of methyl 3,4-dihydroxybenzoate (33) in anhydrous THF (0.5 mL) was added 2 equiv of C²H₃I and Cs₂CO₃, and the mixture was stirred for 72 h. The reaction was quenched with 1 M HCl (0.2 mL), and the product was extracted into ethyl acetate and concentrated under vacuum to yield methyl 3,4-di[C²H₃]methoxybenzoate (34) as a colorless oil, which was dissolved in methanol (300 μL) and mixed with aqueous NaOH (5 M, 0.5 mL). After stirring for 30 min at rt, the reaction was quenched with 1 M HCl, and the product was extracted into ethyl acetate. The separated organic extract was evaporated to yield 3,4-di[C²H₃]methoxybenzoic acid (14) as a white solid (Scheme 8).

Computational Methods. All QM calculations were performed using the Gaussian 03W program package. The predicted structures of reactants, dissociation products, and transition states were optimized using the B3LYP exchange-correlation function and the 6-311++G(d,p) basis set. Calculated stationary states were confirmed to be either ground states or transition states by vibrational frequency analysis. Calculated electronic energies of stationary states were corrected for the zero-point vibrational energy (ZPE), and the ZPE corrections were scaled by a factor of 0.9877.³⁵ Gibbs free energy values were calculated assuming a temperature of 298 K and a pressure of 1 Pa in the collision cell. Unimolecular rate constants (*k*) were calculated from the Gibbs free energy differences between transition states and the reactants (Δ*G*[‡]) using the following equation.³⁶

$$k = \frac{k_B T}{h} \exp\left(-\frac{\Delta G^\ddagger}{RT}\right)$$

where *k_B* is the Boltzmann constant; *h* is Planck's constant; *R* is the gas constant; *T* is the temperature, and Δ*G*[‡] is the Gibbs free energy difference between a transition state and a reactant

■ ASSOCIATED CONTENT

■ Supporting Information

Atom coordinates and absolute energies of structures in Figures 5 and 6, and copies of ¹H and ¹³C NMR spectra for new compounds. This material is available free of charge via the Internet at <http://pubs.acs.org>.

■ AUTHOR INFORMATION

Corresponding Author

*E-mail: athula.attygalle@stevens.edu

Notes

The authors declare no competing financial interest.

■ ACKNOWLEDGMENTS

This research was supported by funds provided by Stevens Institute of Technology (Hoboken, NJ) and Merck Research Laboratories (Rahway, NJ). We thank Bristol-Myers Squibb (New Brunswick, NJ) for the donation of the Quattro Ultima mass spectrometer.

■ REFERENCES

- (1) Cole, R. B. *Electrospray and MALDI Mass Spectrometry: Fundamentals, Instrumentation, Practicalities, and Biological Applications*; John Wiley & Sons: Hoboken, NJ, 2010.
- (2) Hill, A. W.; Mortishire-Smith, R. J. *Rapid Commun. Mass Spectrom.* **2005**, *19*, 3111–3118.
- (3) HighChem, Ltd. <http://www.highchem.com> (accessed 2013).

(4) Attygalle, A. B.; Garcia-Rubio, S.; Ta, J.; Meinwald, J. J. *Chem. Society, Perkin Trans. 2* **2001**, 498–506.

(5) Attygalle, A. B.; Bialecki, J. B.; Nishshanka, U.; Weisbecker, C. S.; Ruzicka, J. J. *Mass Spectrom.* **2008**, *43*, 1224–1234.

(6) Chowdhury, D.; Maurya, S.; Pandey, M. B.; Sarma, B. K.; Singh, U. P. *Mycobiology* **2005**, *33*, 206–209.

(7) Majmudar, C. Y.; Højfeldt, J. W.; Arevang, C. J.; Pomerantz, W. C.; Gagnon, J. K.; Schultz, P. J.; Cesa, L. C.; Doss, C. H.; Rowe, S. P.; Vsquez, V.; Tamayo-Castillo, G.; Cierpicki, T.; Charles, L.; Brooks, C. L.; Sherman, D. H.; Mapp, A. K. *Angew. Chem., Int. Ed.* **2012**, *51*, 11258–11262.

(8) Kitahara, N.; Endo, A.; Furuya, K.; Takahashi, S. J. *Antibiot. (Tokyo)* **1981**, *34*, 1562–1568.

(9) Minkin, V. I.; Minyaev, R. M.; Dorogan, I. V. *J. Mol. Struct.: THEOCHEM* **1997**, *398/398*, 237–253.

(10) Bulo, R. E.; Jansen, H.; Ehlers, A. W.; Kanter, F. J. J.; Schakel, M.; Lutz, M.; Spek, A. L.; Lammertsma, K. *Angew. Chem., Int. Ed.* **2004**, *43*, 714–714.

(11) Dorogan, I. V.; Minkin, V. I.; Novikova, L.; Mendeleev, M. *Chem. Commun.* **2003**, *13*, 205–207.

(12) Lavorato, D. J.; Terlouw, J. K.; McGibbon, G. A.; Dargel, T. K.; Koch, W.; Schwarz, H. *Int. J. Mass Spectrom.* **1998**, *179/180*, 7–14.

(13) Bienkowski, T.; Danikiewicz, W. *Rapid Commun. Mass Spectrom.* **2003**, *17*, 697–705.

(14) Ben-Ari, J.; Etinger, A.; Weisz, A.; Mandelbaum, A. *J. Mass Spectrom.* **2005**, *40*, 1064–1071.

(15) Dickstein, J. S.; Curto, J. M.; Gutierrez, O.; Mulrooney, C. A.; Kozłowski, M. C. *J. Org. Chem.* **2013**, *78*, 4744–4761.

(16) Eichinger, P. C. H.; Bowie, J. H.; Hayes, R. N. *Aust. J. Chem.* **1989**, *42*, 865–874.

(17) Kuck, D. *Int. J. Mass Spectrom.* **2002**, *213*, 101–144.

(18) Wenthold, G.; Paulino, J. A.; Squires, R. R. *J. Am. Chem. Soc.* **1991**, *113*, 7414–1715.

(19) Wenthold, P. G.; Squires, R. R. *J. Am. Chem. Soc.* **1994**, *116*, 6401–6412.

(20) Wenthold, P. G.; Hu, J.; Squires, R. R. *J. Am. Chem. Soc.* **1996**, *118*, 11865–11871.

(21) Wenthold, P. G.; Hu, J.; Squires, R. R. *J. Mass Spectrom.* **1998**, *33*, 796–802.

(22) McAnoy, A. M.; Dua, S.; Blanksby, S. J.; Bowie, J. H. *J. Chem. Soc. Perkin Trans. 2* **2000**, 1665–1673.

(23) Koch, H. F. *Acc. Chem. Res.* **1984**, *17*, 137–144.

(24) Crews, P.; Rodrigues, J.; Jaspars, M. *Organic Structure Analysis*; Oxford University Press: New York, 1998.

(25) Karni, M.; Mandelbaum, A. *Org. Mass Spectrom.* **1980**, *15*, 53–64.

(26) Krauss, D.; Maninx, H. G.; Tauscher, B.; Bischof, P. *Org. Mass Spectrom.* **1985**, *20*, 614–618.

(27) Attygalle, A. B.; Ruzicka, J.; Varughese, D.; Bialecki, J. B.; Jafri, S. J. *Mass Spectrom.* **2007**, *42*, 1207–1217.

(28) Hu, N.; Tu, Y.-P.; Jiang, K.; Pan, Y. J. *Org. Chem.* **2010**, *75*, 4244–4250.

(29) Chai, Y.; Hu, N.; Pan, Y. J. *Am. Soc. Mass Spectrom.* **2013**, *24*, 1097–1101.

(30) Zeller, A.; Strassner, Th. *Organometallics* **2002**, *21*, 4950–4954.

(31) Khairallah, G. N.; O'Hair, R. A. J. *Int. J. Mass Spectrom.* **2006**, *254*, 145–151.

(32) Schröder, D.; Semialjac, M.; Schwarz, H. *Int. J. Mass Spectrom.* **2004**, *233*, 103–109.

(33) Kleingeld, J. C.; Nibbering, N. M. M. *Tetrahedron* **1983**, *39*, 4193–4196.

(34) Chang, C.-C.; Axe, F.; Bolgar, M.; Attygalle, A. B. *J. Mass Spectrom.* **2010**, *45*, 1130–1138.

(35) Mercero, J. M.; Matxain, J. M.; Lopez, X.; York, D. M.; Largo, A.; Eriksson, L. A.; Ugalde, J. M. *Int. J. Mass Spectrom.* **2005**, *240*, 37–99.

(36) Ditchfield, R.; Hehre, W. J.; Pople, J. A. *J. Chem. Phys.* **1971**, *54*, 724–728.